

Natural convection in an enclosure with discrete roughness elements on a vertical heated wall

S. SHAKERIN

Mechanical Engineering Department, University of the Pacific, Stockton, CA 95211, U.S.A.

M. BOHN

Solar Energy Research Institute, Golden, CO 80401, U.S.A.

and

R. I. LOEHRKE

Mechanical Engineering Department, Colorado State University, Fort Collins, CO 80523, U.S.A.

(Received 13 April 1987 and in final form 9 December 1987)

Abstract—Laminar natural convection flow next to a heated wall with single and repeated, two-dimensional, rectangular roughness elements is studied numerically and experimentally. Dye flow visualization in water confirms the numerical prediction that the steady flow over these elements does not separate. Although steady flow reversals near the wall are not predicted or observed, nearly stagnant regions are formed, particularly between closely spaced roughness elements. The surface heat flux in these stagnant regions is relatively low, so the total heat transfer rate may be nearly the same as for a smooth wall in spite of the increased surface area.

1. INTRODUCTION

AN UNDERSTANDING of natural convection heat transfer is essential for proper design of building energy systems, particularly for those buildings where passive heating and cooling techniques are employed. Most of the past experimental and analytical work on natural convection heat transfer from surfaces has focused on smooth surfaces. However, the surfaces of buildings are seldom smooth. Based on the results of experiments and analysis in forced convection, one might anticipate that the roughness associated with surface texture and with isolated elements, such as window frames, may significantly influence the overall heat transfer rate from a wall. If this influence can be predicted with a reasonable degree of confidence, then surface treatment may become a design variable for heat transfer control. More fundamental data on the influence of surface roughness on heat transfer coefficients in natural convection are required to assess the magnitude of this effect.

Reference [1] identified two distinctly different ways that the natural convection heat transfer coefficient may be altered by roughness. The roughness may introduce disturbances into an overlying laminar boundary layer, which cause the boundary layer to prematurely undergo transition to turbulence. Thus, that part of the wall exposed to turbulent flow, which in absence of the roughness would have been in laminar flow, experiences heat transfer augmentation. Another way in which heat transfer may be altered is through various mechanisms associated with the

locally altered flow near the roughness element. The heat transfer in fully separated zones may be reduced compared to that at the same location on a smooth surface. On the other hand, local flow acceleration in the attached regions and unsteady vortical flow originating in the unstable separated shear layer downstream of the roughness element may enhance heat transfer.

An early work in this area is that of Eckert *et al.* [2] who used smoke flow visualization to study the effect of a single, rectangular roughness element on the apparent position of transition on a vertical heated plate in air. They reported a decrease in the distance from the leading edge of the plate to the beginning of transition of up to 15% when an element with a height of about three quarters of the boundary layer thickness was added to a smooth plate.

The present work deals with the same fundamental roughness geometry but focuses on the flow and heat transfer processes in an enclosure in the immediate vicinity of single and repeated rectangular elements. Our interest in enclosures stems from the ultimate application mentioned earlier, building heat transfer. Due to stratification and flow recirculation in enclosures, results from classical vertical-plate-in-infinite-medium studies are not immediately applicable.

2. APPROACH

This study was carried out with complementary numerical and experimental efforts. Quantitative pre-

NOMENCLATURE

A	aspect ratio, H/L	V	dimensionless horizontal velocity, vL/α
H	height of test cell	x	vertical dimension
k	thermal conductivity	X	dimensionless space variable, x/L
L	distance between heated and cooled surfaces in the test cell	y	horizontal dimension
l	height of roughness element	Y	dimensionless space variable, y/L .
Nu_L	local Nusselt number, $q''_w L/k(T_H - T_C)$	Greek symbols	
\overline{Nu}_L	average Nusselt number, $\overline{q''_w} L/k(T_H - T_C)$	α	thermal diffusivity
p	distance along wall	β	coefficient of thermal expansion
P	length of heated surface including roughness	δ	boundary layer thickness
Pr	Prandtl number	θ	dimensionless temperature, $(T - T_i)/(T_H - T_C)$
q''_w	local heat flux	ν	kinematic viscosity
$\overline{q''_w}$	average wall heat flux, $(1/H) \int_0^P q''_w dp$	ψ	stream function, $\partial\psi/\partial y = U$, $-\partial\psi/\partial x = V$.
Ra_L	Rayleigh number, $g\beta(T_H - T_C)L^3/\nu\alpha$	Subscripts	
S	spacing between roughness elements	C	cooled wall
T_i	initial fluid temperature for transient calculation, $(T_H + T_C)/2$	H	heated wall
u	vertical velocity	1	lower roughness element
U	dimensionless vertical velocity, uL/α	2	upper roughness element.
v	horizontal velocity		

dictions were obtained over a range of parameters from the numerical part, while the qualitative checks on these predictions and on the validity of the two-dimensional model employed were provided by the experimental part.

2.1. Numerical

The unsteady, two-dimensional Boussinesq equations were solved for the flow in a rectangular enclosure. The equations for vorticity, stream function, and temperature were cast in finite-difference form using forward time differences, centered differences for the diffusive terms, and upwind differences for the convective terms. Each calculation started with the fluid isothermal and at rest. The two side walls were maintained at uniform, constant temperatures above and below the initial fluid temperature and the floor and ceiling of the enclosure were adiabatic. The calculations proceeded in time until steady-state conditions were achieved. A non-uniform, zonal mesh was used with grid points spaced more closely in the boundary layer and around the roughness element than in the core. At least five, and usually seven, grid points were located in the boundary layer. The results were checked for grid independence and, for the case of smooth side walls, against a previously published 'benchmark' solution [3], for enclosure flows. A detailed description of the numerical technique is contained in ref. [4].

The roughness element height l (see Fig. 1 for nomenclature) was chosen to be a multiple of the boundary layer thickness at the center of the smooth-walled enclosure at the same Rayleigh number. The

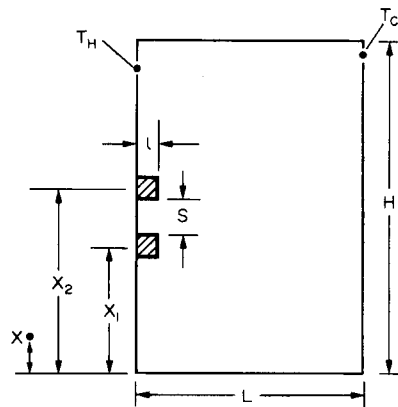


FIG. 1. Nomenclature for enclosure with roughness elements on heated wall.

boundary layer thickness was defined as the distance from the wall to the first zero crossing of the velocity profile. All of the numerical results presented here are for $l/\delta = 1$; however, this study has been extended to $\frac{1}{2} \leq l/\delta \leq 2$ and the results are qualitatively the same. Likewise, most of the results presented here are for an enclosure with aspect ratio $A = H/L = 1$, $Ra_L = 10^6$, $Pr = 0.7$, but the study has included $1 \leq A \leq 3$, $10^5 \leq Ra_L \leq 10^8$, and $Pr = 0.7$ and 7.0 with qualitatively the same results.

2.2. Experimental

Experiments were performed in two different test cells. Dye visualization of the flow over the roughness was carried out in a water-filled 300 mm cubical test

cell. Opposing, smooth vertical aluminum walls were heated and cooled to drive the flow. The other two vertical walls were made of lucite to permit viewing. The roughness elements for this test were 6.3 mm square aluminum rods that were glued to the heated wall using RTV silicone adhesive. The axis of each rod was horizontal, and the rod spanned the entire heated surface. The floor of the test cell was insulated and the top was open to allow insertion of a 1.5 mm diameter dye injection probe. The temperature difference between the hot and cold walls was maintained at 14°C giving a Rayleigh number based on the test cell dimensions of 8.3×10^9 . The temperature uniformity on the heated plate was within $\pm 0.5^\circ\text{C}$. Details of the test cell and estimation of the magnitude of the heat losses are presented in ref. [5].

The second experimental apparatus used in this study included an air-filled enclosure and a Mach-Zehnder interferometer with a 150 mm diameter field of view. The opposing, active aluminum walls of the enclosure were 510 mm wide and 1110 mm high and were separated by 310 mm. The remaining surfaces of the enclosure were insulated lucite. Moveable optical windows, placed at opposite sides of the heated plate, exposed the boundary layer to one of the interferometer beams. A detailed description of this apparatus is contained in ref. [6]. For the purpose of the tests reported here the enclosure side walls (except for the windows) were insulated externally while the floor and ceiling were insulated internally. The internal rigid foam insulation reduced the height of the walls to 910 mm creating an enclosure with an aspect ratio of 3; the hot and cold wall of the enclosure were maintained at 40 and 11°C, respectively, yielding a Rayleigh number of $Ra_L = 5.3 \times 10^7$ based on the span between the active plates.

The roughness elements for this test were 12.5 mm square aluminum bar stock attached to the heated wall with RTV silicone adhesive. The heated wall was maintained at a uniform temperature to within $\pm 0.5^\circ\text{C}$ using individually controlled electric heater strips. Thermocouples attached to a roughness element indicated that heat conduction through the adhesive was sufficient to keep the element at the same temperature (within $\pm 0.5^\circ\text{C}$) as the hot wall.

3. RESULTS

3.1. Flow field

The flow fields around single and repeated roughness elements were studied numerically and experimentally in the water tank. Dye injection at the base of the heated wall showed that the flow, in the absence of the roughness element, was steady in the lower half of the enclosure. Somewhat above the center of the wall the dye streak lines became sinusoidally distorted and rolled up into vortices before reaching the upper surface.

The flow over a single roughness placed at $X_1/H = \frac{1}{4}$ (see Fig. 1) remained steady and two-dimensional.

The local Rayleigh number at this position was $Ra_{X_1} = 1.3 \times 10^8$. Dye injection into the boundary layer below the rod rose along the wall and followed the contour of the roughness. Separation, with reverse flow at the wall or at the surface of the roughness, was never observed in the experiments provided that the element was located where the flow over the smooth wall was steady. Instantaneous flow reversal and shedding from the rod were observed only when the flow approaching the rod was unsteady. Numerical calculations confirm the absence of flow reversal in steady state for elements attached to the wall of an enclosure. Instantaneous flow reversal above the roughness is predicted only at early times in the start-up transient.

The tenacious nature of the boundary layer is vividly demonstrated in the flow over two closely spaced elements. The flow with $S = 2l$ is shown in Fig. 2. In Fig. 2(a) the dye introduced near the wall below the elements follows the wall and indicates the unidirectional nature of the flow. The dye in Fig. 2(b) was introduced near the maximum velocity point and shows that the main flow dips in near the wall between the two elements. A similar set of streak lines is shown in Fig. 3 for rods set at $S = l$. Here, the main flow bridges the gap between the rods but the flow inside the gap does not reverse.

Similar quantitative results from the numerical calculations are shown in Fig. 4 for the flow in a square enclosure at $Ra_L = 10^6$ for $S = l$ in Fig. 4(a) and $S = 2l$ in Fig. 4(b). The boundary layers are relatively thick, so the roughness elements are large. The flow in the entire enclosure is steady; the flow in the vicinity of the roughness is similar to that visualized in the water tank.

3.2. Heat transfer

The influence of a single roughness on the boundary layer heat transfer can be seen from the distortion of the isotherms. The calculated isotherm pattern in an enclosure of $A = 1$ and $Ra_L = 10^8$ is shown in Fig. 5. A closeup view of the roughness element and isotherms on the wall of the air-filled enclosure is shown in the interferogram in Fig. 6. This element is attached at $X_1/H = \frac{1}{4}$ so $Ra_{X_1} = 2.2 \times 10^7$. Both the calculated and measured isotherm patterns indicate that the surface heat flux is reduced along the wall just below and just above the element compared with what it would be on a smooth wall. The temperature gradient at the outer surface of the element appears to be high, especially near the lower, outside corner.

These observations are quantified in Fig. 7, where the local Nusselt number, based on the calculated isotherms, is plotted as a function of position along the surface. The magnitude of the Nusselt number on the rough surface is indicated by the distance between the surface and the solid curved lines. The dashed line indicates the Nusselt number along the smooth wall at the same Rayleigh number. It can be seen that the influence of the roughness is mainly localized to within

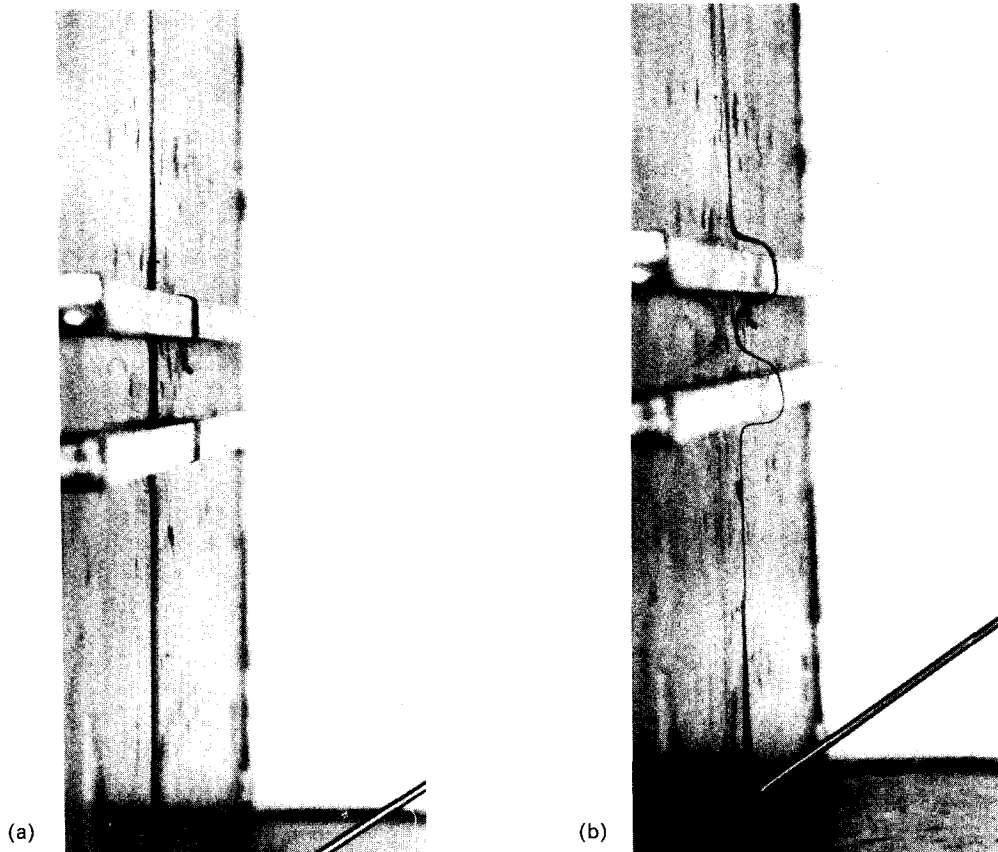


FIG. 2. Dye visualization of flow over two bars, $S = 2l$: (a) dye injected near wall; (b) dye streak near velocity maximum.

about two roughness heights above and below the roughness location. It also appears from this plot that the heat transferred through the extra surface area added by the roughness (the horizontal surfaces) should just about balance the reduction in heat transferred from the wall immediately below and above the element. This observation turns out to be roughly correct, as can be verified for $Ra_L = 10^6$ by comparing the first two entries in Table 1. Here, the average Nusselt number \overline{Nu}_L over the entire heated surface is presented for several geometries. This Nusselt number is based on the total heat transfer rate from the heated surface and can therefore be used as a direct measure of this influence of the roughness on overall heat transfer from a surface. The increase in \overline{Nu}_L , shown in Table 1, for a single roughness compared to a smooth wall is 12%. This is much smaller than the 32% increase in surface area due to the addition of a single roughness at this Rayleigh number.

The interferograms for double roughness elements are shown in Fig. 8 indicate that for closely spaced elements the heat transfer from the surfaces that make up the cavity between the elements should be relatively low. Similar conditions are shown in Fig. 9 for the calculated isotherms for two elements in an enclosure with $Ra_L = 10^6$. The addition of a second roughness with $S = l$ results in no change in \overline{Nu}_L from that for

a single roughness at $Ra_L = 10^6$. This can be verified by comparing the second and third entries in Table 1. If the spacing between the two elements is increased to $S = 2l$, then \overline{Nu}_L increases slightly.

The average \overline{Nu}_L for a single rectangular roughness element with an overall length (up the plate) equal to the sum of the two square roughness elements plus the gap between them is also shown in Table 1. The near equality of the average \overline{Nu}_L for the cases of two elements with $S = l$ and for the rectangular element with length $3l$ shows that at this close spacing the total heat transfer rate from the three surfaces of length l forming the cavity between two roughness elements is essentially equal to that from a single surface of length l positioned near the boundary layer.

4. DISCUSSION AND CONCLUSIONS

Eckert *et al.* [2] interpreted the existence of steady smoke streak lines over their obstacle as an indication that a flow-separation bubble existed with a steady laminar rotation within the separated flow region. This phenomenon was not observed in the present study: steady separation with reversal of wall shear stress was never observed in the two-dimensional flow over square rods. The steady natural convection

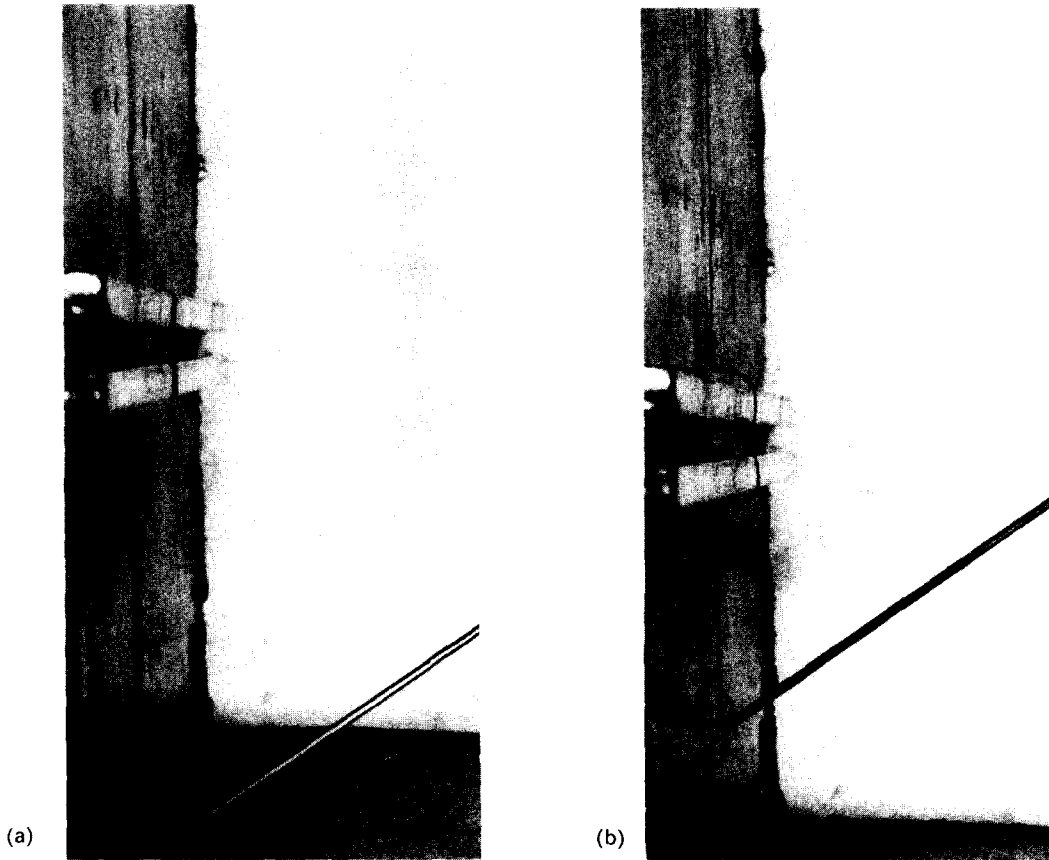


FIG. 3. Dye flow visualization for two bars, $S = l$: (a) dye injected near wall; (b) dye streak near velocity maximum.

boundary layers studied here tend to follow the wall contour very closely. The main boundary-layer flow skips over the gap between closely spaced roughnesses, but even here the slowly moving fluid between elements follows the main boundary layer. A recently published, two-dimensional, numerical study by Oos-

thuisen and Paul [7] indicates that this conclusion concerning the absence of separation may hold even for large surface interruptions that extend horizontally nearly from wall to wall. However, boundary layers flowing over *large* heated horizontal surfaces (or under cooled surfaces) are likely to become three-

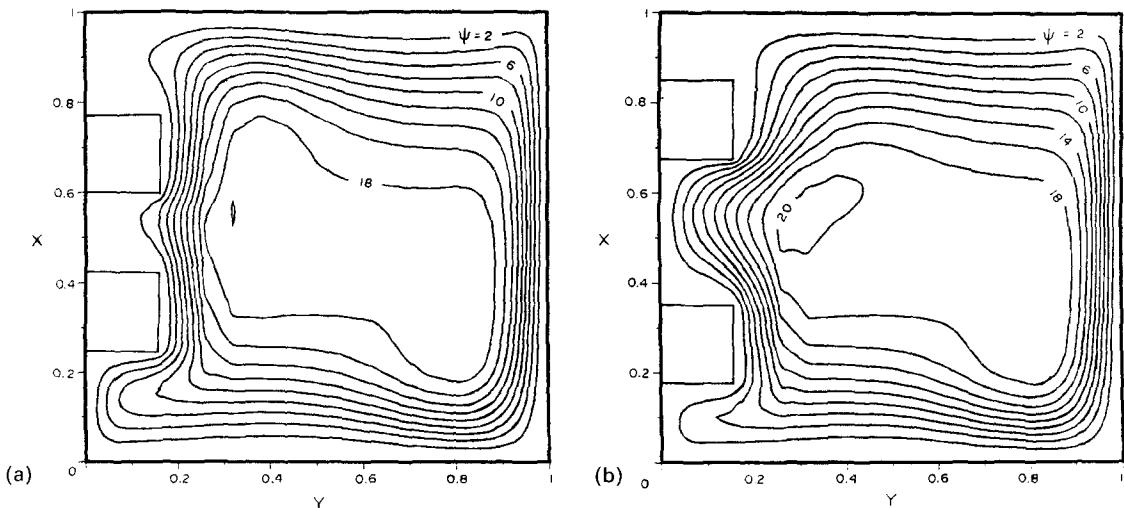


FIG. 4. Calculated streamlines for flow over two roughness elements in an enclosure, $A = 1$, $Ra_l = 10^6$, $Pr = 0.72$: (a) $S = l$; (b) $S = 2l$.

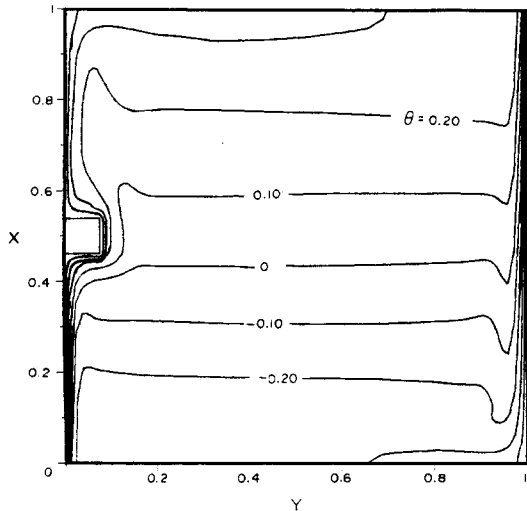


FIG. 5. Calculated isotherms for flow over single roughness element in an enclosure, $A = 1$, $Ra_L = 10^8$, $Pr = 0.72$.

dimensional so the range of validity of these calculations needs to be further defined.

Heat transfer augmentation may be obtained in forced convection by placing a two-dimensional roughness element, such as one of the rods used in this study, in a laminar boundary layer. The highly unstable, separated shear layer created in the flow over a single rod undergoes rapid transition to turbulence and may augment heat transfer for a considerable distance downstream from the obstacle. The experiments reported here indicate that this mechanism for heat transfer augmentation is not so powerful in natural convection.

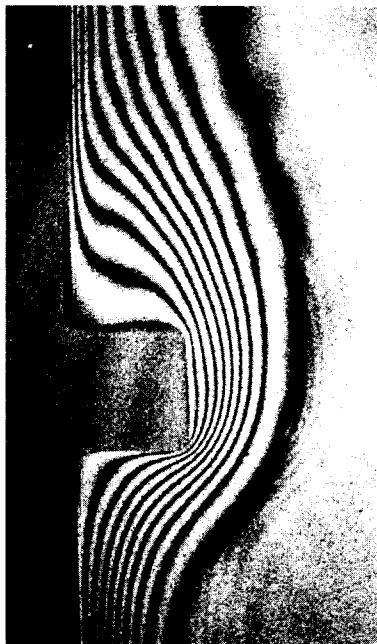


FIG. 6. Interferogram showing isotherms around a single roughness element in an enclosure, $Ra_{X_1} = 2.2 \times 10^7$, $Pr = 0.71$.

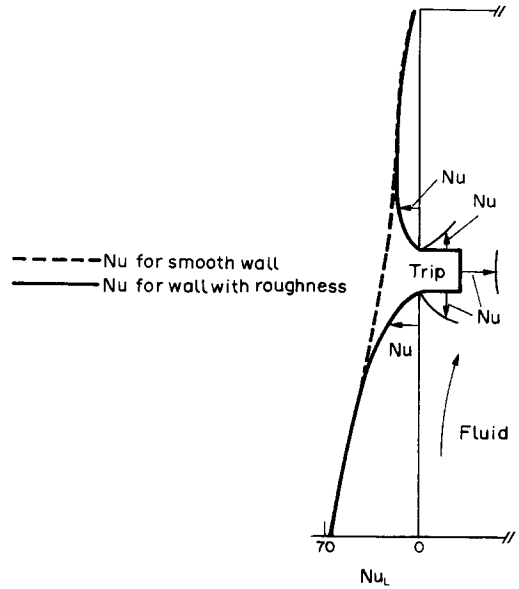


FIG. 7. Calculated local Nusselt number for flow on a heated wall in an enclosure with and without a roughness element, $A = 1$, $Ra_L = 10^8$, $Pr = 0.72$.

The effect of a roughness element on the downstream flow field and heat transfer was not studied in the present work. However, Eckert *et al.* [2] have concluded, on the basis of flow visualization, that the transition point may be displaced upstream by about 15% because of a two-dimensional roughness. The influence of this displacement of the transition point on heat transfer needs further clarification.

Heat transfer may also be augmented by the addition of discrete roughness elements to a wall simply because the total surface area is increased. The results of the calculations reported here show that in laminar flow, a single horizontal bar is a poor fin even if it is perfectly conducting. The gain caused by added surface area is just about cancelled by the reduction in heat transfer coefficient because of the turning of the boundary layer. With conducting, closely spaced, multiple roughness elements the total heat transfer is not significantly different from that for a smooth surface.

Table 1. Influence of geometry on the total heat transfer rate from the heated surface of an enclosure ($A = 1$, $Ra_L = 10^6$, $Pr = 0.72$)

Geometry of heated surface	\overline{Nu}_L
Smooth surface	9.2
Single roughness	10.3
Double roughness:	
$S = l$	10.3
$S = 2l$	10.7
Rectangular roughness:	
length = $3l$	10.2
length = $4l$	10.3

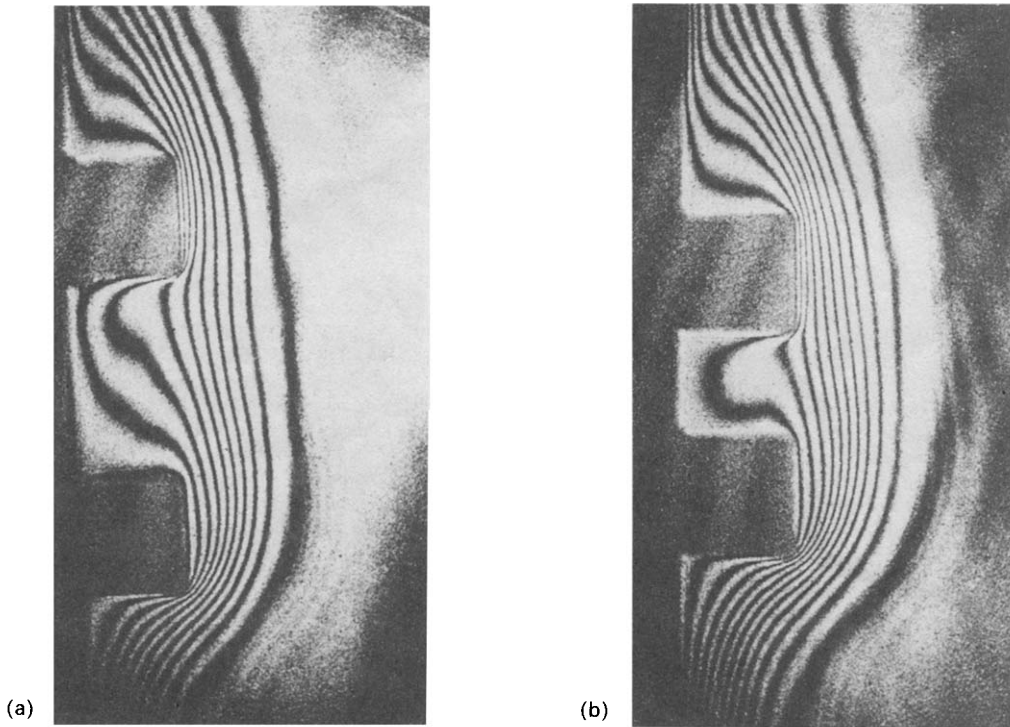


FIG. 8. Interferograms for two roughness elements in an enclosure, $Ra_{\gamma_1} = 2.2 \times 10^7$, $Pr = 0.71$: (a) $S = 2l$; (b) $S = l$.

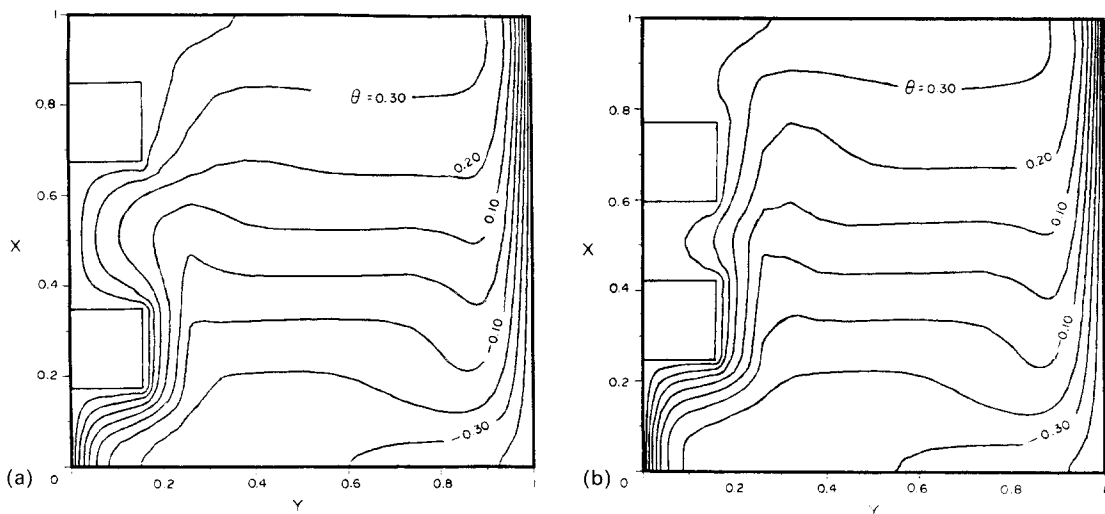


FIG. 9. Calculated isotherms in an enclosure with two roughness elements, $A = 1$, $Ra_L = 10^6$, $Pr = 0.72$: (a) $S = 2l$; (b) $S = l$.

Acknowledgements—Computer time on the CYBER 205 was generously provided by the Institute for Computational Studies at CSU. This work was partially funded by the Office of Solar Heat Technology of the U.S. Department of Energy as part of the Solar Buildings Technologies Program. The third author received support for participation in the experimental part of this work that was performed at SERI from the Associated Western Universities, Inc.

REFERENCES

1. R. Anderson and M. Bohn, Heat-transfer enhancement in natural convection enclosure flow, *J. Heat Transfer* **108**, 330-336 (1986).
2. E. R. G. Eckert, J. P. Hartnett and T. F. Irvine, Jr., Flow-visualization studies of transition to turbulence in free-convection flow, ASME Paper 60-W-250 (1960).

3. G. de Vahl Davis, Natural convection of air in a square cavity: a bench mark numerical solution, *Int. J. Numer. Meth. Fluids* **3**, 249–264 (1983).
4. S. Shakerin, Laminar natural convection on a vertical surface with discrete roughness, Ph.D. Thesis, Colorado State University, Fort Collins, Colorado (1986).
5. M. Bohn, A. Kirkpatrick and P. Olson, Experimental study of three dimensional natural convection at high Rayleigh numbers, *J. Heat Transfer* **106**, 339–345 (1984).
6. M. Bohn, E. Fisher and R. Anderson, Development of an interferometer for natural convection enhancement research, SERI/PR-252-2598, Solar Energy Research Institute, Golden, Colorado (1985).
7. P. H. Oosthuizen and J. T. Paul, Free convection heat transfer in a cavity fitted with a horizontal plate on the cold wall. In *Advances in Enhanced Heat Transfer* (Edited by S. M. Shenkman *et al.*), HTD 43, pp. 101–207. ASME (1985).

CONVECTION NATURELLE DANS UNE CAVITE AVEC ELEMENTS DE RUGOSITE SUR UNE PAROI VERTICALE CHAUDE

Résumé—On étudie numériquement et expérimentalement la convection naturelle laminaire proche d'une paroi chaude avec des éléments rectangulaires répétitifs de rugosité. Une visualisation dans l'eau confirme le calcul numérique qui prédit que l'écoulement permanent sur ces éléments ne se sépare pas. Bien que des renversements d'écoulement ne sont ni prédits ni observés, des régions presque immobiles sont formées particulièrement entre des éléments de rugosité très rapprochés. Le flux de chaleur surfacique dans ces régions stagnantes est relativement faible, si bien que le flux total est à peu près le même que pour une paroi lisse en dépit de l'accroissement de surface.

NATÜRLICHE KONVEKTION IN EINEM HOHLRAUM MIT KÜNSTLICHEN RAUHEITSELEMENTEN AN EINER SENKRECHT BEHEIZTEN WAND

Zusammenfassung—Die laminare Strömung durch natürliche Konvektion in der Nähe einer beheizten Wand mit wiederholt angebrachten, einzelnen zweidimensionalen rechtwinkligen Rauheitselementen wurde numerisch und experimentell untersucht. Sichtbarmachung der Strömung in Wasser mit einer Farbmarkierung bekräftigte die numerische Aussage, daß sich die ausgebildete Strömung an diesen Elementen nicht ablöst. Obwohl keine Rückströmung in Wandnähe vorausgesagt oder beobachtet wurde, bildeten sich Zonen aus, in denen die Strömung nahezu stagniert, besonders zwischen dichtstehenden Rauheitselementen. Die Oberflächenwärmestromdichte ist in diesen Ruheregionen ziemlich klein, so daß der gesamte Wärmestrom beinahe derselbe ist wie an einer glatten Wand—trotz der vergrößerten Oberfläche.

ЕСТЕСТВЕННАЯ КОНВЕКЦИЯ В ПОЛОСТИ С ДИСКРЕТНЫМИ ЭЛЕМЕНТАМИ ШЕРОХОВАТОСТИ НА ВЕРТИКАЛЬНОЙ НАГРЕТОЙ СТЕНКЕ

Аннотация—Численно и экспериментально изучается ламинарное естественноконвективное течение возле нагретой стенки с одиночными и повторяющимися двумерными прямоугольными элементами шероховатости. Наблюдение подкрашенного течения воды подтверждает выводы, полученные в результате численного расчета, о том, что устойчивость течения не нарушается над этими элементами. Хотя устойчивые возвратные потоки над элементами шероховатости не были получены в расчетах и не наблюдались, зато образовывались практически застойные зоны, особенно между близко расположенными элементами шероховатости. Тепловой поток через поверхность в застойных зонах был относительно низок, поэтому общая интенсивность теплопереноса оказалась почти такой же, как в случае гладкой стенки, несмотря на возросшую площадь поверхности.